Phospholipid flippases enable precursor B cells to flee engulfment by macrophages

Katsumori Segawa[a], Yuichi Yanagihashi[a], Kyoko Yamada[a], Chigure Suzuki[b], Yasuo Uchiyama[c], and Shigekazu Nagata[a,1]

[a]Laboratory of Biochemistry & Immunology, World Premier International Research Center, Immunology Frontier Research Center, Osaka University, 565-0871, Osaka, Japan; [b]Department of Cellular and Molecular Pharmacology, Juntendo University Graduate School of Medicine, 113-8421 Tokyo, Japan; and [c]Department of Cellular and Neuropathology, Juntendo University Graduate School of Medicine, 113-8421 Tokyo, Japan

Contributed by Shigekazu Nagata, September 28, 2018 (sent for review August 21, 2018; reviewed by Suzanne Cory and Patrick Williamson)

ATP11A and ATP11C, members of the P4-ATPases, are flippases that translocate phosphatidylserine (PtdSer) from the outer to inner leaflet of the plasma membrane. Using the W3 T lymphoma cell line, we found that Ca^{2+} ionophore-induced phospholipid scrambling caused prolonged PtdSer exposure in cells lacking both the *ATP11A* and *ATP11C* genes. *ATP11C*-null (*ATP11C*$^{-/y}$) mutant mice exhibit severe B-cell deficiency. In wild-type mice, ATP11C was expressed at all B-cell developmental stages, while ATP11A was not expressed after pro−B-cell stages, indicating that *ATP11C*$^{-/y}$ early B-cell progenitors lacked plasma membrane flippases. The receptor kinases MerTK and Axl are known to be essential for the PtdSer-mediated engulfment of apoptotic cells by macrophages. *MerTK*$^{-/-}$ and *Axl*$^{-/-}$ double deficiency fully rescued the lymphopenia in the *ATP11C*$^{-/y}$ bone marrow. Many of the rescued *ATP11C*$^{-/y}$ pre-B and immature B cells exposed PtdSer, and these cells were engulfed alive by wild-type peritoneal macrophages, in a PtdSer-dependent manner. These results indicate that ATP11A and ATP11C in precursor B cells are essential for rapidly internalizing PtdSer from the cell surface to prevent the cells' engulfment by macrophages.

flippase | lymphopenia | phosphatidylserine | macrophages | entosis

Phospholipids are asymmetrically distributed between the lipid bilayer of plasma membranes in eukaryotic cells. Aminophospholipids such as phosphatidylserine (PtdSer) and phosphatidylethanolamine (PtdEtn) are confined to the inner leaflet, whereas 60 to 70% of the phosphatidylcholine and sphingomyelin is in the outer leaflet (1). This asymmetrical distribution is important for plasma membrane integrity, signal transduction cascades, and cell shape, but is irreversibly disrupted when cells undergo apoptosis, during which PtdSer is exposed on the cell surface, and functions as an "eat me" signal to macrophages (2). Macrophages then engulf these apoptotic cells via Tyro3−Axl−MerTK (TAM) receptor kinases, with the help of PtdSer-binding proteins such as Protein S, Gas6, and Tim4 (2).

At least two enzyme systems, flippases and scramblases, regulate the phospholipid dynamics at the plasma membrane (1, 3). Among the 14 to 15 members of the P4-type ATPases, ATP11A and ATP11C, together with their chaperone CDC50A at the plasma membrane, function as flippases that specifically translocate PtdSer and PtdEtn from the outer to inner leaflet using ATP (4–6). ATP11A and ATP11C are cleaved by caspase 3, which irreversibly inactivates them.

Two families of proteins (TMEM16 and XKR) function as scramblases, which quickly disrupt the asymmetrical distribution of phospholipids by providing nonspecific pathways for phospholipid transport between the plasma membrane leaflets (7). In mouse, TMEM16F is ubiquitously expressed in various cells, and functions as a Ca^{2+}-activated phospholipid scramblase in a homodimeric form (8, 9), and Xkr8 forms a heterodimer with its chaperone Basigin or Neuroplastin, and functions as a scramblase after being cleaved by caspase 3 (10, 11). Thus, when cells such as platelets and lymphocytes are activated, the intracellular Ca^{2+} concentration increases, which transiently activates the TMEM16F scramblase, inducing transient PtdSer exposure. On the other hand, when cells undergo apoptosis, caspase 3 cleaves ATP11A/ATP11C and Xkr8, thereby both irreversibly inactivating the flippases and activating the scramblase, thus quickly exposing PtdSer in an irreversible fashion (3, 7). We proposed that the irreversible exposure of PtdSer due to flippase inactivation is necessary for its role as an "eat me" signal (2).

The ATP11C gene is located on mouse X chromosome, and, in 2011, two groups independently identified *ATP11C*-null mutant (*ATP11*$^{-/y}$) mice by the genetic screening of *N*-ethyl-*N*-nitrosourea (ENU)-treated founders for low $CD19^+$ B cells in the blood (12, 13). The mutant mice exhibited B-cell lymphopenia in the blood, but not T-cell lymphopenia, and suffered from mild anemia, cholestasis, and dystocia (12–16). In particular, the numbers of $CD24^{hi}CD43^-$ pre-B, IgD^-IgM^+ immature B, and IgD^+IgM^+ mature B cells in the *ATP11C*$^{-/y}$ bone marrow were 1 to 10% of those in wild-type mice. Although a reduction in flippase activity was detected in various hematopoietic cells in the *ATP11C*$^{-/y}$ mice (16), how the loss of ATP11C caused these phenotypes remained elusive.

Here we report that ATP11A and ATP11C are important for rapidly reestablishing the asymmetrical PtdSer distribution after it is exposed to the cell surface by Ca^{2+}-dependent scramblase. The bone marrow B-cell progenitors stop expressing ATP11A after the pre−pro-B-cell stage, and these B-cell progenitors in *ATP11C*-null mice expose PtdSer due to a lack of flippase and are engulfed alive by macrophages in a PtdSer-dependent manner.

Results

Rapid Internalization of PtdSer by ATP11A and ATP11C. To examine the contribution of ATP11A and 11C to PtdSer's translocation at the plasma membrane, the *ATP11A* and *11C* genes in mouse T-cell

Significance

ATP11A and ATP11C are P4-type ATPases that function redundantly as phospholipid flippases at the plasma membrane, and a deficiency in ATP11C causes B-cell lymphopenia. Here we show that flippases at the plasma membrane are important for quickly internalizing phosphatidylserine (PtdSer) that is exposed by Ca^{2+}-dependent scramblase in activated cells. During development, B-cell progenitors in the bone marrow stop expressing ATP11A, and *ATP11C*-null B-cell progenitors expose PtdSer. The PtdSer is recognized as an "eat me" signal by bone marrow macrophages for entosis, which is the engulfment of live cells, explaining why the lack of a flippase causes B-cell lymphopenia.

Author contributions: K.S. and S.N. designed research; K.S., Y.Y., K.Y., and C.S. performed research; K.S., Y.Y., C.S., Y.U., and S.N. analyzed data; and K.S. and S.N. wrote the paper.

Reviewers: S.C., Walter and Eliza Hall Institute; and P.W., Amherst College.

Conflict of interest statement: K.Y. is on a leave of absence from Chugai Pharmaceutical Co.

See Commentary on page 12092.

[1]To whom correspondence should be addressed. Email: snagata@ifrec.osaka-u.ac.jp.

This article contains supporting information online at www.pnas.org/lookup/suppl/doi:10.1073/pnas.1814323115/-/DCSupplemental.

Published online October 24, 2018.

lymphoma W3 cells were knocked out individually or together by the CRISPR–Cas9 system (*SI Appendix*, Fig. S1). As shown in Fig. 1*A*, the PtdSer flippase activity in *ATP11A*$^{-/-}$ cells, measured by the incorporation of 1-oleoyl-2-{6-[(7-nitro-2-1,3-benzoxadiazol-4-yl)amino]hexanoyl}-*sn*-glycero-3-phosphoserine (NBD-PS), a fluorescently labeled PtdSer, was slightly lower than that in wild-type cells, while that in *ATP11C*$^{-/-}$ cells was less than 20% of the wild-type activity. These results were consistent with the findings that the ATP11C mRNA in W3 cells was 2 to 3 times more abundant than that of ATP11A (*SI Appendix*, Fig. S2), and that the PtdSer-supported ATPase activity of ATP11C is ∼40% stronger than that of ATP11A (4). The double mutation of *ATP11A* and *11C* resulted in flippase activity that was about 12% that of wild type (Fig. 1*A*), yet the *ATP11A*$^{-/-}$*ATP11C*$^{-/-}$ W3 cells did not constitutively expose PtdSer on their surface (*SI Appendix*, Fig. S3). Since ATP11A and 11C are the only P4-ATPases that function as PtdSer flippases on the plasma membrane of W3 cells (4), this observation suggested that another system(s) exists for establishing the asymmetric distribution of PtdSer in the long-term steady-state condition.

We next examined the contribution of ATP11A and 11C to reestablishing the asymmetrical PtdSer distribution after scramblase-induced PtdSer exposure. Treating W3 cells with A23187, a Ca^{2+} ionophore, rapidly exposed PtdSer (Fig. 1*B*) by the action of TMEM16F (9). When the A23187 was removed, the PtdSer disappeared from the surface within 10 min, indicating that flippases rapidly translocated it from the outer to inner plasma membrane leaflet. This reestablishment of the PtdSer distribution was little affected by the null mutation of *ATP11A*, but was strongly compromised by the defect in *ATP11C*. W3 cells lacking both *ATP11A* and *11C* (*DKO*) genes lost their ability to reestablish the asymmetrical PtdSer distribution, at least within 10 min. GFP-tagged ATP11A or ATP11C expressed in *DKO* W3 cells was localized to the plasma membrane, and had strong flippase activity to internalize NBD-PS (Fig. 1*C*). Accordingly, the expression of either ATP11A or ATP11C fully rescued the ability of *DKO* cells to rapidly reestablish the asymmetrical distribution of PtdSer after Ca^{2+} ionophore-induced PtdSer exposure (Fig. 1*D*). These results indicated that ATP11A and ATP11C have redundant roles in reestablishing the asymmetrical distribution of PtdSer in the plasma membrane.

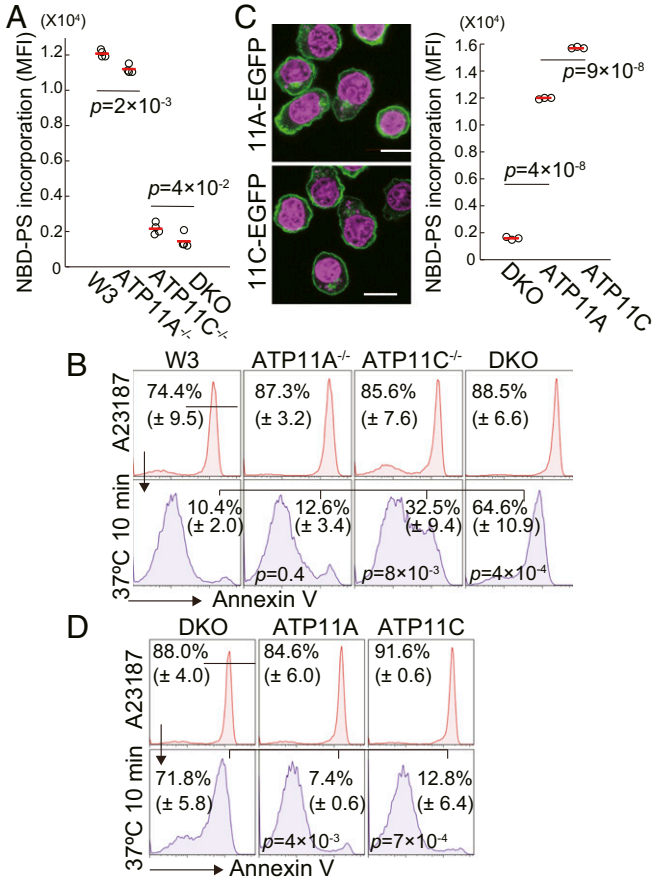

Fig. 1. Rapid internalization of PtdSer by ATP11A and 11C. (*A*) Wild-type (W3), *ATP11A*$^{-/-}$, *ATP11C*$^{-/-}$, and *ATP11A*$^{-/-}$*ATP11C*$^{-/-}$ (*DKO*) cells were incubated with NBD-PS, and analyzed by flow cytometry. Incorporated NBD-PS was expressed as median fluorescence intensity (MFI). Experiments were performed in triplicate. Horizontal bars indicate average values. *P* values are shown. (*B*) W3, *11A*$^{-/-}$, *11C*$^{-/-}$, and *DKO* cells were treated for 6 min with A23187. A portion of the cells was immediately analyzed for PtdSer exposure (*Upper*), while the remaining cells were incubated at 37 °C for 10 min in RPMI1640 containing 10% FBS-2 mM EGTA before flow cytometry (*Lower*). Experiments were performed three times, and the average percentage of Annexin V$^+$ cells in the PI$^-$ population is indicated with SD. (*C*) *DKO* cells were transformed with GFP- ATP11A or 11C, and observed by confocal microscopy (*Left*). Green, EGFP; magenta, DRAQ5. (Scale bar, 10 μm.) The 11A and 11C transformants were incubated at 20 °C for 5 min with NBD-PS, and analyzed by flow cytometry (*Right*). Incorporated NBD-PS was expressed as MFI. Horizontal bars denote average values ($n = 3$). (*D*) *DKO*, 11A-DKO, and 11C-DKO cells were treated with A23187. A portion of the cells was immediately analyzed for PtdSer exposure (*Upper*), while the remaining cells were incubated at 37 °C for 10 min without A23187 before flow cytometry (*Lower*). Experiments were performed three times, and the average percentage of Annexin V$^+$ cells in the PI$^-$ population is indicated with SD.

Nonredundant Role of ATP11C in B-Cell Precursors. *ATP11C*$^{-/y}$ mice exhibit pleiotropic phenotypes, including B lymphopenia, anemia, dystocia, and cholestasis (12–15). We confirmed that, although the total number of bone marrow cells was similar between wild-type and *ATP11C*$^{-/y}$ mice, the numbers of pre-B, immature B cells, and mature B cells was severely reduced in the *ATP11C*$^{-/y}$ mice (Fig. 2*A*). The percentage of pre–pro-B and pro-B cells was increased from 11.2 to 50.5% and 9.5 to 34%, respectively, in these mice, indicating that B-cell development was blocked at the pro-B stage. In contrast, the number of mature and immature T cells ($CD4^{-/-}CD8^{-/-}$, $CD4^+CD8^+$, $CD4^+CD8^-$, and $CD4^-CD8^+$ thymocytes) in the thymus was normal (Fig. 2*A*). Since ATP11A and 11C act redundantly to flip PtdSer (Fig. 1), we hypothesized that T cells express both ATP11A and 11C, while B cells express only ATP11C. To examine this possibility, we sorted B- and T-cell progenitors from bone marrow cells and thymocytes, respectively, and measured the ATP11A and 11C mRNA levels by real-time RT-PCR. As shown in Fig. 2*B*, all of the T-cell subsets expressed both the ATP11A and 11C mRNAs, while there was little ATP11A mRNA in the bone marrow pro-B, pre-B, immature B, or mature B cells. Accordingly, the *ATP11C* deficiency reduced the PtdSer flippase activity of $B220^+IgD^-$ B-cell progenitors by 65% (Fig. 2*C*). These results suggested that *ATP11C*$^{-/y}$ B cells lose their flippase activity at the pro-B, pre-B, and immature B-cell stages.

Possible Mechanisms for the B-Cell Lymphopenia in *ATP11C*$^{-/y}$ Mice. We previously showed that, when viable W3 cells completely lack flippase activity due to a CDC50A deficiency, they are engulfed by macrophages in a PtdSer-dependent manner (5). Thus, we speculated that live B-cell progenitors in *ATP11C*$^{-/y}$ mice were engulfed by macrophages in the bone marrow, resulting in B-cell lymphopenia.

Macrophages use various molecules when engulfing PtdSer-exposing apoptotic cells (efferocytosis). Among them, either MerTK or Axl is required for efficient efferocytosis together with Tim4, a PtdSer receptor (17). Grün et al. (18) recently performed single-cell RNA sequencing with mouse bone marrow cells. Analysis of the data set (Gene Expression Omnibus accession no. GSE76983) revealed two clusters (clusters 25 and 32) of cells expressing F4/80, CD68, MerTK, Axl, and Tim4 (*SI Appendix*, Table S1), indicating

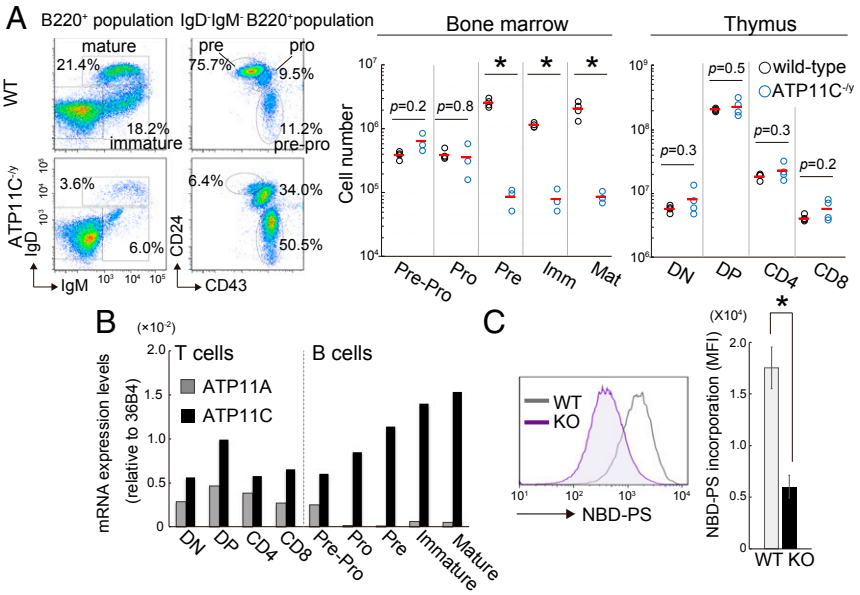

Fig. 2. No redundant activity for ATP11C in B-cell progenitors. (*A*) Bone marrow cells from wild-type or *ATP11C*$^{-/y}$ mice were stained for B220, IgD, IgM, CD24, and CD43 (*Left*). Staining profiles in the B220^{+} and IgD^{-}IgM^{-}B220^{+} populations are shown. Numbers indicate percentages of IgD^{+}IgM^{+} (mature), IgD^{-}IgM^{+} (immature), CD24^{hi}CD43^{-} (pre-B), CD24^{int}CD43^{+} (pro-B), and CD24^{-}CD43^{+} (pre-pro) B cells. Number of respective bone marrow B-cell subsets per femur (*Center*), or T-cell subsets per thymus (*Right*) (n = 3 to 4). Horizontal bars denote averages. *P < 0.007. (*B*) RNA of the indicated bone marrow B-cell and thymus T-cell subsets from three 8-wk-old C57BL/6J male mice was subjected to real-time RT-PCR for ATP11A and 11C mRNAs. The mRNA level relative to that of 36B4 ribosomal protein is shown. (*C*) Bone marrow cells from wild-type (WT) and *ATP11C*$^{-/y}$ (KO) mice were stained for B220 and IgD, incubated at 20 °C with NBD-PS for 10 min, and analyzed by flow cytometry. Experiment was performed with three different mice, and the mean value of the incorporated NBD-PS (MFI) was plotted with SD. *P value < 0.003.

that certain subsets of bone marrow macrophages express MerTK, Axl, and Tim4. Our immunohistochemical analysis also showed that Axl^{+}MerTK^{+}Tim4^{+}F4/80^{+} macrophages were present throughout the bone marrow (*SI Appendix*, Fig. S4).

Rescue of B-Cell Lymphopenia in *ATP11C*$^{-/y}$ Mice by Deficiencies in TAM Receptors. To examine whether PtdSer-expressing B cells were engulfed by macrophages, wild-type and *ATP11C*$^{-/y}$ littermates were treated twice a day for 4.5 d with 40 mg/kg of BMS-777607, an inhibitor of TAM-family kinases (19). As shown in Fig. 3, BMS-777607 treatment of wild-type mice slightly reduced the number of all B-cell progenitor subsets in the bone marrow. Since the MerTK and Axl mRNAs were not expressed in B-cell progenitors (*SI Appendix*, Fig. S5), this adverse effect of BMS-777607 was probably due to its inhibition of other tyrosine kinases (19). However, the administration of BMS-777607 into *ATP11C*$^{-/y}$ mice markedly increased the numbers of pre-B and immature B cells, but not of mature B cells, to levels comparable to those in the BMS-777607–treated wild-type littermates.

To confirm that MerTK and Axl were involved in the bone marrow B-cell lymphopenia, *ATP11C*$^{-/y}$ mice were crossed with *MerTK*$^{-/-}$*Axl*$^{-/-}$ mice (*DKO*), to establish *ATP11C*$^{-/y}$*MerTK*$^{-/-}$, *ATP11C*$^{-/y}$*Axl*$^{-/-}$, and *ATP11C*$^{-/y}$*MerTK*$^{-/-}$*Axl*$^{-/-}$ (*TKO*) mice. Consistent with the lack of MerTK and Axl expression in the B-cell progenitors, the single or double deficiency of the *MerTK* and *Axl* genes had little effect on the B-cell development in *ATP11C*-intact (*ATP11C*$^{+/y}$) mice (Table 1 and *SI Appendix*, Fig. S6). In contrast, the *MerTK* or *Axl* deficiency markedly increased the number of pre-B, immature B, and mature B cells in the *ATP11C*$^{-/y}$ bone marrow. The percentage of pre-B cells in the *ATP11C*$^{-/y}$ bone marrow increased from 8.3 to 28.5% in the *MerTK*$^{-/-}$, to 47.0% in the *Axl*$^{-/-}$, and to 58.1% in the *MerTK*$^{-/-}$*Axl*$^{-/-}$ background. The total cell number of the respective progenitors in the bone marrow also increased (Table 1 and *SI Appendix*, Fig. S6). The numbers of B-cell progenitors in the bone marrow in *MerTK*$^{-/-}$*Axl*$^{-/-}$*ATP11C*$^{-/y}$ mice were comparable to those in wild-type mice. On the other hand, although the B-cell lymphopenia (221 cells per microliter) in the periphery of *ATP11C*$^{-/y}$ mice was significantly improved to 754 cells per microliter by the double deficiency of *MerTK* and *Axl* (Table 1), this number was still only 18% of that in the periphery of wild-type (*ATP11C*$^{+/y}$) mice.

Engulfment of Viable *ATP11C*$^{-/y}$ B-Cell Progenitors by Macrophages. Since the *ATP11C*$^{-/y}$ pre-B, immature B, and mature B cells in the bone marrow were dramatically increased by the double deficiency of *MerTK* and *Axl*, which are involved in PtdSer-dependent efferocytosis, we examined the PtdSer exposure in B-cell progenitors. As reported previously (20), 10 to 20% of the freshly isolated progenitor B cells exposed PtdSer, and this proportion

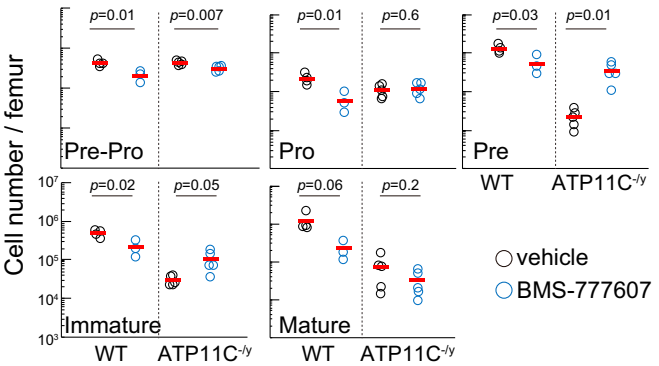

Fig. 3. Effect of a TAM-receptor inhibitor on bone marrow B-cell lymphopenia. WT and *ATP11C*$^{-/y}$ mice were injected with BMS-777607. The number of B-cell subsets per femur at 5 h to 6 h after the last injection was plotted. Experiments were performed with three to five mice for each genotype, and average values are shown by a horizontal line. *P* values are shown.

Table 1. Rescue of the B-cell lymphopenia in *ATP11C*$^{-/y}$ mice by the loss of MerTK and Axl

Genotype			Number of B cells in bone marrow or in peripheral blood*					
ATP11C	*MerTK*	*Axl*	Pre−pro-B (×10^5)	Pro-B (×10^5)	Pre-B (×10^5)	Immat B (×10^5)	Mat B (×10^5)	Peri B (×10^6)
WT	Wt/Ht	Wt/Ht	3.9 ± 0.5	3.0 ± 0.5	17.0 ± 2.6	7.2 ± 0.3	17.0 ± 3.0	6.9 ± 1.6
Ambr	Wt/Ht	Wt/Ht	4.1 ± 0.7	1.9 ± 0.5	0.6 ± 0.2	0.5 ± 0.2	3.7 ± 1.8	0.2 ± 0.1
WT	KO	Wt/Ht	2.6 ± 0.2	3.3 ± 0.9	18.0 ± 2.7	8.1 ± 1.1	12.0 ± 2.0	4.3 ± 0.6
Ambr	KO	Wt/Ht	3.2 ± 0.8	2.2 ± 0.8	2.5 ± 1.2	1.2 ± 0.2	12.0 ± 5.8	0.3 ± 0.1
Wt	Wt/Ht	KO	2.9 ± 0.9	2.9 ± 1.1	14.0 ± 5.0	5.3 ± 1.6	8.6 ± 2.1	3.7 ± 0.1
Ambr	Wt/Ht	KO	2.9 ± 0.3	2.8 ± 0.6	6.2 ± 3.0	2.4 ± 1.2	7.0 ± 2.4	0.8 ± 0.3
WT	KO	KO	3.0 ± 0.8	2.8 ± 0.6	16.0 ± 3.6	6.4 ± 2.1	12.0 ± 6.4	4.3 ± 1.3
Ambr	KO	KO	4.0 ± 1.2	2.2 ± 0.7	10.0 ± 4.8	4.3 ± 2.0	14.0 ± 8.1	0.8 ± 0.1

*Male *ATP11C*$^{+/y}$*Axl*$^{-/+}$*MerTK*$^{-/-}$, *ATP11C*$^{+/y}$*Axl*$^{-/-}$*MerTK*$^{+/-}$, or *ATP11C*$^{+/y}$*Axl*$^{+/+}$*MerTK*$^{+/+}$ mice were crossed with female *ATP11C*$^{+/-}$*Axl*$^{-/-}$*MerTK*$^{-/-}$ or *ATP11C*$^{+/-}$*Axl*$^{+/-}$*MerTK*$^{+/-}$ mice, and analyses were carried out with male littermates. Numbers of pre−pro-B, pro-B, pre-B, immature B (Immat B), and mature B (Mat B) in B220$^+$PI$^-$ bone marrow cells per femur, and peripheral blood B220$^+$ cells (Peri B) per milliliter in the SYTOX Blue$^-$ population, are shown. Three to seven mice for each group were analyzed, and the mean values are shown with SD. Ht, heterozygous; KO, knock-out; WT, wild-type.

was increased by the *ATP11C* deficiency to about 30% of the pro-B cells and 50% of the pre-B and immature B cells (Fig. 4*A*). The *MerTK*$^{-/-}$*Axl*$^{-/-}$ mutation (DKO) increased the percentage of PtdSer-exposing pro-B cells (30.7 to 49.4%). On the other hand, the same mutation had little effect on the percentage of PtdSer-exposing pre-B and immature B cells (around 50%) in the *ATP11C*$^{-/y}$ mice, but increased the numbers of these cells 3.8 to 17.5 times. Electron microscopy observation indicated that more than 80% of these PtdSer-exposing precursor B cells (B220$^+$IgD$^-$ cells) from the *ATP11C*$^{-/y}$*MerTK*$^{-/-}$ *Axl*$^{-/-}$ mice were not apoptotic or necrotic (Fig. 4*B*). In contrast to the precursor B cells, the mature B cells of the *ATP11C*$^{-/y}$ bone marrow did not expose PtdSer, but their number increased 3.8 times by the *MerTK* and *Axl* double mutation. These results suggested that the activated PtdSer-exposing *ATP11C*$^{-/y}$ pre-B and immature B cells were left unengulfed in the *MerTK*$^{-/-}$*Axl*$^{-/-}$ bone marrow, and that the PtdSer was subsequently internalized via an ATP11A/ATP11C-independent mechanism.

To confirm that the PtdSer-exposing B-cell progenitors were engulfed by macrophages in an Axl- or MerTK-dependent manner, B-cell progenitors (B220$^+$IgD$^-$ cells) were prepared from *MerTK*$^{-/-}$*Axl*$^{-/-}$*ATP11C*$^{+/y}$ or *MerTK*$^{-/-}$*Axl*$^{-/-}$*ATP11C*$^{-/y}$ bone marrow, among which 30 to 40% of the *ATP11C*$^{-/y}$ progenitors exposed PtdSer (*SI Appendix*, Fig. S7). These B-cell progenitors were labeled with pHrodo and incubated with resident peritoneal macrophages. As shown in Fig. 4 *C* and *D* and Movie S1, *ATP11C*$^{-/y}$ B cells were efficiently engulfed by the macrophages. This engulfment was not observed with *MerTK*$^{-/-}$*Axl*$^{-/-}$ macrophages, and was inhibited by the D89E mutant of milk fat globule EGF factor 8 (MFG-E8), which masks PtdSer (21). The percentage of pHrodo-positive macrophages was 7.9% after incubation with wild-type B-cell progenitors, suggesting that apoptotic B cells present in the culture were engulfed. This percentage increased to 30.2% after incubation with *ATP11C*$^{-/y}$ B-cell progenitors. Since more than 80% of the *ATP11C*$^{-/y}$ B-cell progenitors were alive, these results indicated that most of the pHrodo-positive macrophages had engulfed live cells. Electron microscopy showed that the wild-type peritoneal macrophages that had engulfed *ATP11C*$^{-/y}$ cells had an intact or swollen morphology (Fig. 4*E*), a characteristic of live-cell engulfment, or entosis (22), whereas the engulfed apoptotic cells exhibited condensed nuclei. Of the macrophages engulfing *ATP11C*$^{-/y}$ B-cell progenitors, 75% (15/20) carried swollen or intact cells, and 25% (5/20) carried cells with condensed nuclei. Furthermore, observation of the bone marrow of *ATP11C*$^{-/y}$ mice by electron microscopy revealed peculiar macrophages carrying degenerated cellular components (Fig. 4*F*), which were not present in the wild-type bone marrow. Together, these results suggested that the PtdSer-exposing B progenitors were engulfed alive by macrophages in vivo.

Discussion

ATP11C-null mice exhibit severe B-cell lymphopenia by a previously unknown mechanism (12, 13). Here we found that this B-cell lymphopenia can be explained in part by the PtdSer-dependent entosis of B-cell progenitors.

We found that bone marrow precursor B cells lose their ATP11A after the pre−pro-B-cell stage. During B-cell development in the bone marrow, the expression of a set of genes is epigenetically regulated (23). Since a CpG island in the *ATP11A* gene is a target for methylation (24), it is possible that the *ATP11A* gene suppression in B-cell progenitors is due to DNA methylation. B cells are selected at multiple checkpoints during their maturation process, in a manner controlled by their B-cell receptor (BCR) repertoire, which determines their self-recognition or immune response functions (25). According to Dillon et al. (20), a small population of viable B-cell progenitors (pre-B and immature B) that may have undergone positive selection expose PtdSer. We confirmed this finding, and showed that *ATP11C* deficiency greatly increased the PtdSer-exposing population in B-cell progenitors. Since the engagement of BCR increases the intracellular Ca^{2+} concentration (26), it is possible that signaling from a pre-BCR or BCR activates B-cell progenitors to expose PtdSer via Ca^{2+}-dependent scramblase. In wild-type mice, ATP11C would internalize PtdSer, while, in *ATP11C*$^{-/y}$ B-cell progenitors, once PtdSer was exposed to the cell surface, it would not be internalized.

We previously reported that viable cells that expose PtdSer due to the constitutive activation of Ca^{2+}-dependent scramblase (TMEM16F) are not engulfed by macrophages (27). Here, we showed that B-cell progenitors lacking flippase stably exposed PtdSer, and were engulfed by macrophages. The number of B-cell progenitors was abruptly reduced at the pre−B-cell stage, at which a large number of precursor B cells normally undergo apoptosis and are engulfed by macrophages (25), suggesting that PtdSer-exposing live pre-B cells were also recognized by macrophages at this stage. Henson et al. (28) previously proposed that viable cells present a "don't eat me" signal on their surface. Mouse red blood cells and human leukemia cells express CD47, which is proposed to function as a "don't eat me" signal (29). Real-time RT-PCR indicated that all of the mouse B-cell progenitors expressed a high level of CD47 mRNA, and FACS analysis revealed that the surface CD47 protein level was similar between wild-type and *ATP11C*$^{-/y}$ B-cell progenitors, and much higher than that on mature red blood cells (*SI Appendix*, Fig. S8). These results indicated that the CD47 expressed on B-cell progenitors was nonfunctional as a "don't eat me" signal, or that the PtdSer "eat me" signal could overcome the CD47 "don't eat me" signal for the entosis of B-cell progenitors. This agrees with the previous results obtained with resealed erythrocytes (30)

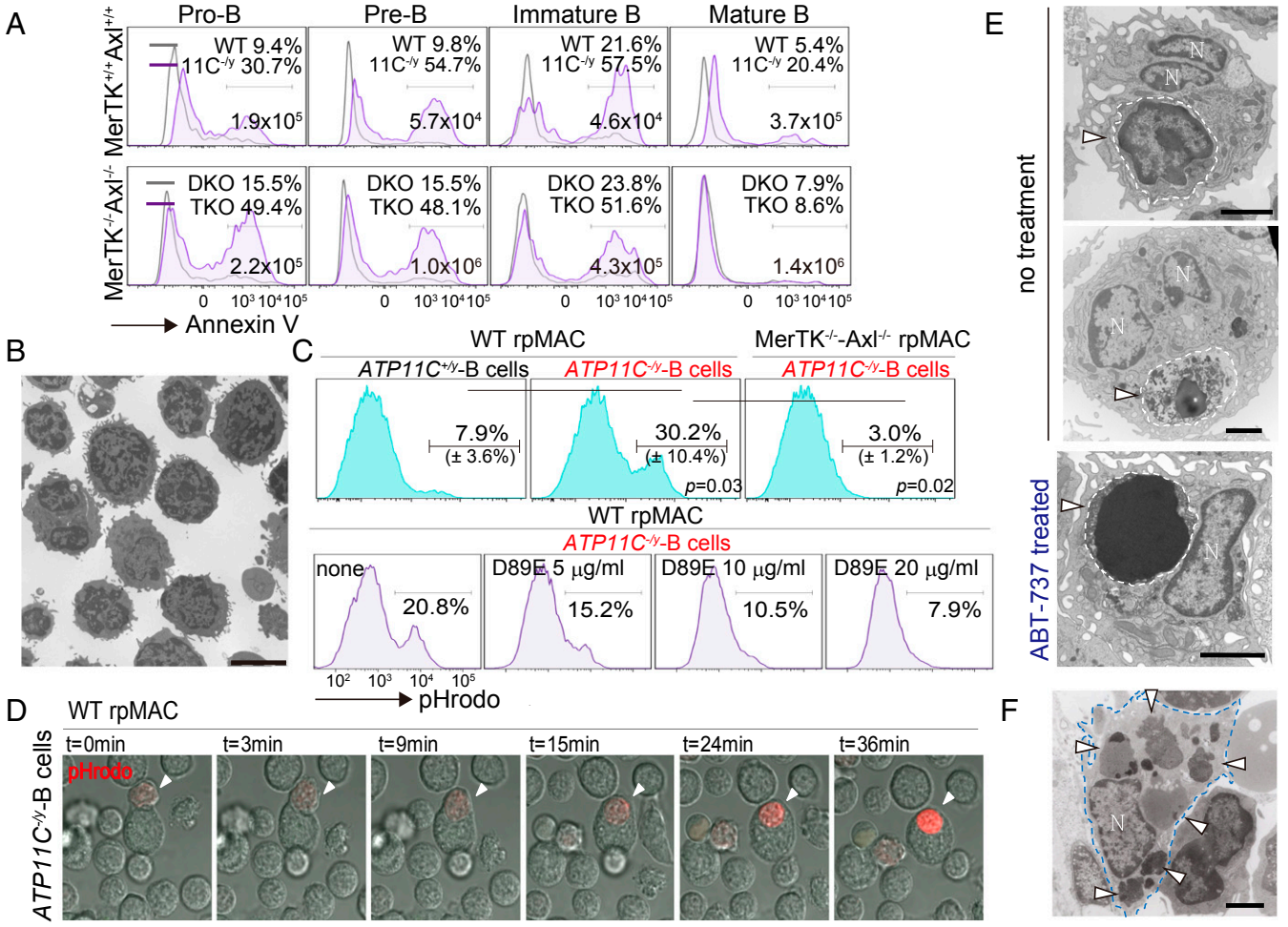

Fig. 4. Entosis of *ATP11C*$^{-/y}$ B-cell progenitors. (*A*) Bone marrow cells from 11-wk-old WT and *ATP11C*$^{-/y}$ (*Upper*), *ATP11C*$^{+/y}$ *MerTK*$^{-/-}$*Axl*$^{-/-}$ (DKO), and *ATP11C*$^{-/y}$ *MerTK*$^{-/-}$*Axl*$^{-/-}$ (TKO) (*Lower*) male mice were stained for B220, IgD, IgM, CD24, and CD43, together with Annexin V and 7-AAD. Annexin V profiles of pro-B, pre-B, immature B, and mature B cells in the 7-AAD^{-} population are shown. Numbers denote the percentages of 7-AAD^{-}Annexin V^{+} cells. Average cell numbers for each B-cell progenitor per femur are shown. (*B*) The PI^{-}Annexin V^{+} IgD^{-}B220^{+} bone marrow cells from *ATP11C*$^{-/y}$*MerTK*$^{-/-}$*Axl*$^{-/-}$ mice were observed by transmission electron microscopy. (Scale bar, 5 μm.) (*C*) IgD^{-}B220^{+} B cells from the bone marrow of *ATP11C*$^{+/y}$ or *ATP11C*$^{-/y}$ mice were labeled with pHrodo, and incubated with WT or *MerTK*$^{-/-}$*Axl*$^{-/-}$ resident peritoneal macrophages (rpMac) (*Upper*). Histograms for pHrodo in CD11b^{+} macrophages are shown. Experiments were performed three to four times using different mice, and the average percentage of pHrodo^{+} cells is shown with SD. *P* values are shown. *ATP11C*$^{-/y}$ B-cell progenitors were incubated with wild-type rpMacs in the presence of the indicated concentration of D89E (*Lower*). (*D*) Time-lapse images of entosis. The pHrodo-B cell progenitors from *ATP11C*$^{-/y}$ mice were incubated with wild-type rpMacs. Images for pHrodo (Red) and DIC were captured every 2 min to 3 min. Arrowheads indicate engulfed B cells. (*E*) PI^{-} B cells from *ATP11C*$^{-/y}$ bone marrow were incubated with wild-type rpMac, and observed by electron microscopy (*Upper*). As a control, the macrophages engulfing ABT737-treated B cell progenitors were observed (*Lower*). Arrowheads indicate engulfed living or apoptotic B cells. N denotes macrophage nucleus. (Scale bar, 2 μm.) (*F*) Femurs from *ATP11C*$^{-/y}$ mice were decalcified and fixed with paraformaldehyde. Sections were observed by electron microscopy. A macrophage containing engulfed materials is highlighted. Arrowheads indicate degenerated cellular materials. (Scale bar, 2 μm.)

Like apoptotic T cells in the thymus (31), the apoptotic PtdSer-exposing B cells cannot be detected in the bone marrow, probably due to their swift efferocytosis. However, live PtdSer-exposing B-cell progenitors, particularly in the *ATP11C*-null background, were detected, suggesting that the entosis of B-cell progenitors may not be as efficient as their efferocytosis. Apoptotic cells secrete a variety of chemotactic molecules, such as lysophosphatidylcholine, ATP, and UTP, as "find me" signals (32). It is unlikely that live B-cell progenitors produce such chemotactic signals, which may explain the inefficient entosis of the B-cell progenitors. Similarly, the different localization and activation state of B-cell progenitors (25) may also explain why the PtdSer-exposing pre-B but not pro-B cells undergo entosis.

The B-cell lymphopenia in the bone marrow of *ATP11C*$^{-/y}$ mice was almost fully recovered by double mutation of the *Axl* and *MerTK* genes. The peripheral B-cell number was increased threefold by these mutations, but it was still about 5 to 6 times lower than that of wild-type mice. In addition to B-cell lymphopenia, *ATP11C*$^{-/y}$ mice suffer from anemia and cholestasis (12–15), which were not rescued by the loss of MerTK and Axl. Yabas et al. (15) reported that *ATP11C*$^{-/y}$ erythrocytes develop normally, but the mature erythrocytes have an abnormal shape and a shortened life span. The *ATP11C*-null mutation also downregulates bile salt transporters in hepatocytes, leading to a defect in the uptake of unconjugated bile salts (33, 34). Mouse erythrocytes and hepatocytes do not express ATP11A (BloodSpot, servers.binf.ku.dk/bloodspot/; BioGPS, biogps.org), indicating that *ATP11C*$^{-/y}$ erythrocytes and hepatocytes would lack PtdSer-flippase activity. As previously discussed (35, 36), a lack of flippase may affect the rigidity and fluidity of the plasma membrane, inducing an abnormal cell shape and vulnerability to mechanical stress. It is possible that *ATP11C*$^{-/y}$ erythrocytes are damaged

during circulation due to their vulnerability. This may also explain why the peripheral B-cell lymphopenia was not fully rescued by the *MerTK* and *Axl* mutations.

We showed here that one of physiological functions of the plasma membrane PtdSer flippases is to quickly internalize PtdSer in activated cells to prevent their entosis. A high PtdSer level was maintained for at least 10 min on the surface of the $ATP11A^{-/-}ATP11C^{-/-}$ cells, but eventually disappeared from the cell surface. Although $CDC50A^{-/-}$ cells constitutively expose PtdSer (5), the $ATP11A^{-/-}ATP11C^{-/-}$ cells did not, suggesting that other proteins requiring CDC50A as a chaperone contributed to the asymmetrical distribution of PtdSer at the plasma membrane. In *Saccharomyces cerevisiae*, which does not have PtdSer flippases at its plasma membrane, P4-ATPases at the trans-Golgi network are thought to be responsible for restricting PtdSer to the cytosolic leaflet of the plasma membrane (37, 38). Several mammalian P4-ATPases are localized to the Golgi and/or to recycling endosomes (4, 7). Whether these P4-ATPases or any other molecules contribute to the asymmetrical distribution of PtdSer at the plasma membrane remains to be studied. Finally, entosis or cell cannibalism is found in various biological and pathological processes, such as embryo implantation to the uterus, metastatic tumor cells, and hemophagocytic syndrome (22, 39, 40). It would be interesting to study whether flippase dysfunction or PtdSer exposure is involved in these processes.

Materials and Methods

Mice. C57BL/6J mice were from Japan Central Laboratory for Experimental Animals. $ATP11C^{-/y}$ mice in B6 (12) were from the Mutant Mouse Resource & Research Centers repository, and $Axl^{-/-}$ and $MerTK^{-/-}$ mice in B6/129 mixed background (41) were from Jackson Laboratory. $Axl^{-/-}MerTK^{-/-}$ and $ATP11C^{-/y}Axl^{-/-}MerTK^{-/-}$ mice were generated by crossing $ATP11C^{-/y}$, $Axl^{-/-}$, and $MerTK^{-/-}$ mice. All mice were housed in a specific pathogen-free facility at Research Institute for Microbial Diseases, Osaka University, and all mouse studies were approved by the Ethics Review Committee for Animal Experimentation of Research Institute for Microbial Diseases, Osaka University.

Statistical Analysis. All data were expressed as the mean with SD. Differences between groups were examined for statistical significance using Student's *t* test. Full details for *Materials and Methods* are in *SI Appendix, Extended Materials and Methods*.

ACKNOWLEDGMENTS. We thank H. Omori (Research Institute for Microbial Diseases, Osaka University) for electron microscopy, M. Kubokawa (Amelieff) for bioinformatics, K. Hasegawa for mouse maintenance, and M. Fujii for secretarial assistance. This work was supported by Japan Society for the Promotion of Science (JSPS) Grants-in-Aid for Scientific Research (C) 15K08266 (to K.S.) and for Scientific Research on Innovative Areas 16H01360 and 17H05506 (to K.S.), JSPS Grant-in-Aid for Scientific Research (S) for the Promotion of Science 15H05785 (to S.N.), and Core Research for Evolutional Science and Technology from Japan Science and Technology Agency JPMJCR14M4 (to S.N.).

1. Bevers EM, Williamson PL (2016) Getting to the outer leaflet: Physiology of phosphatidylserine exposure at the plasma membrane. *Physiol Rev* 96:605–645.
2. Nagata S (2018) Apoptosis and clearance of apoptotic cells. *Annu Rev Immunol* 36:489–517.
3. Segawa K, Nagata S (2015) An apoptotic 'eat me' signal: Phosphatidylserine exposure. *Trends Cell Biol* 25:639–650.
4. Segawa K, Kurata S, Nagata S (2016) Human type IV P-type ATPases that work as plasma membrane phospholipid flippases and their regulation by caspase and calcium. *J Biol Chem* 291:762–772.
5. Segawa K, et al. (2014) Caspase-mediated cleavage of phospholipid flippase for apoptotic phosphatidylserine exposure. *Science* 344:1164–1168.
6. Segawa K, Kurata S, Nagata S (2018) The CDC50A extracellular domain is required for forming a functional complex with and chaperoning phospholipid flippases to the plasma membrane. *J Biol Chem* 293:2172–2182.
7. Nagata S, Suzuki J, Segawa K, Fujii T (2016) Exposure of phosphatidylserine on the cell surface. *Cell Death Differ* 23:952–961.
8. Suzuki J, et al. (2013) Calcium-dependent phospholipid scramblase activity of TMEM16 protein family members. *J Biol Chem* 288:13305–13316.
9. Suzuki J, Umeda M, Sims PJ, Nagata S (2010) Calcium-dependent phospholipid scrambling by TMEM16F. *Nature* 468:834–838.
10. Suzuki J, Denning DP, Imanishi E, Horvitz HR, Nagata S (2013) Xk-related protein 8 and CED-8 promote phosphatidylserine exposure in apoptotic cells. *Science* 341:403–406.
11. Suzuki J, Imanishi E, Nagata S (2016) Xkr8 phospholipid scrambling complex in apoptotic phosphatidylserine exposure. *Proc Natl Acad Sci USA* 113:9509–9514.
12. Yabas M, et al. (2011) ATP11C is critical for the internalization of phosphatidylserine and differentiation of B lymphocytes. *Nat Immunol* 12:441–449.
13. Siggs OM, et al. (2011) The P4-type ATPase ATP11C is essential for B lymphopoiesis in adult bone marrow. *Nat Immunol* 12:434–440.
14. Siggs OM, Schnabl B, Webb B, Beutler B (2011) X-linked cholestasis in mouse due to mutations of the P4-ATPase ATP11C. *Proc Natl Acad Sci USA* 108:7890–7895.
15. Yabas M, et al. (2014) Mice deficient in the putative phospholipid flippase ATP11C exhibit altered erythrocyte shape, anemia, and reduced erythrocyte life span. *J Biol Chem* 289:19531–19537.
16. Yabas M, Jing W, Shafik S, Bröer S, Enders A (2016) ATP11C facilitates phospholipid translocation across the plasma membrane of all leukocytes. *PLoS One* 11:e0146774.
17. Yanagihashi Y, Segawa K, Maeda R, Nabeshima YI, Nagata S (2017) Mouse macrophages show different requirements for phosphatidylserine receptor Tim4 in efferocytosis. *Proc Natl Acad Sci USA* 114:8800–8805.
18. Grün D, et al. (2016) De novo prediction of stem cell identity using single-cell transcriptome data. *Cell Stem Cell* 19:266–277.
19. Schroeder GM, et al. (2009) Discovery of N-(4-(2-amino-3-chloropyridin-4-yloxy)-3-fluorophenyl)-4-ethoxy-1-(4-fluorophenyl)-2-oxo-1,2-dihydropyridine-3-carboxamide (BMS-777607), a selective and orally efficacious inhibitor of the Met kinase superfamily. *J Med Chem* 52:1251–1254.
20. Dillon SR, Constantinescu A, Schlissel MS (2001) Annexin V binds to positively selected B cells. *J Immunol* 166:58–71.
21. Hanayama R, et al. (2002) Identification of a factor that links apoptotic cells to phagocytes. *Nature* 417:182–187.
22. Overholtzer M, Brugge JS (2008) The cell biology of cell-in-cell structures. *Nat Rev Mol Cell Biol* 9:796–809.
23. Kulis M, et al. (2015) Whole-genome fingerprint of the DNA methylome during human B cell differentiation. *Nat Genet* 47:746–756.
24. Zhao S, et al. (2017) Epigenome-wide tumor DNA methylation profiling identifies novel prognostic biomarkers of metastatic-lethal progression in men diagnosed with clinically localized prostate cancer. *Clin Cancer Res* 23:311–319.
25. Melchers F (2015) Checkpoints that control B cell development. *J Clin Invest* 125:2203–2210.
26. Baba Y, Kurosaki T (2016) Role of Calcium signaling in B cell activation and biology. *Curr Top Microbiol Immunol* 393:143–174.
27. Segawa K, Suzuki J, Nagata S (2011) Constitutive exposure of phosphatidylserine on viable cells. *Proc Natl Acad Sci USA* 108:19246–19251.
28. Henson PM, Bratton DL, Fadok VA (2001) Apoptotic cell removal. *Curr Biol* 11:R795–R805.
29. Matlung HL, Szilagyi K, Barclay NA, van den Berg TK (2017) The CD47-SIRPα signaling axis as an innate immune checkpoint in cancer. *Immunol Rev* 276:145–164.
30. Pradhan D, Williamson P, Schlegel RA (1994) Phosphatidylserine vesicles inhibit phagocytosis of erythrocytes with a symmetric transbilayer distribution of phospholipids. *Mol Membr Biol* 11:181–187.
31. Surh CD, Sprent J (1994) T-cell apoptosis detected *in situ* during positive and negative selection in the thymus. *Nature* 372:100–103.
32. Medina CB, Ravichandran KS (2016) Do not let death do us part: 'find-me' signals in communication between dying cells and the phagocytes. *Cell Death Differ* 23:979–989.
33. Matsuzaka Y, Hayashi H, Kusuhara H (2015) Impaired hepatic uptake by organic anion-transporting polypeptides is associated with hyperbilirubinemia and hypercholanemia in Atp11c mutant mice. *Mol Pharmacol* 88:1085–1092.
34. de Waart DR, et al. (2016) ATP11C targets basolateral bile salt transporter proteins in mouse central hepatocytes. *Hepatology* 64:161–174.
35. Devaux PF, Herrmann A, Ohlwein N, Kozlov MM (2008) How lipid flippases can modulate membrane structure. *Biochim Biophys Acta* 1778:1591–1600.
36. Lemmon MA (2008) Membrane recognition by phospholipid-binding domains. *Nat Rev Mol Cell Biol* 9:99–111.
37. Andersen JP, et al. (2016) P4-ATPases as phospholipid flippases—Structure, function, and enigmas. *Front Physiol* 7:275.
38. Chen S, et al. (2006) Roles for the Drs2p-Cdc50p complex in protein transport and phosphatidylserine asymmetry of the yeast plasma membrane. *Traffic* 7:1503–1517.
39. Janka GE, Lehmberg K (2014) Hemophagocytic syndromes—An update. *Blood Rev* 28:135–142.
40. Durgan J, Florey O (2018) Cancer cell cannibalism: Multiple triggers emerge for entosis. *Biochim Biophys Acta Mol Cell Res* 1865:831–841.
41. Lu Q, et al. (1999) Tyro-3 family receptors are essential regulators of mammalian spermatogenesis. *Nature* 398:723–728.